On the Insertion Reactions of $CH_2(\tilde{a}\,^1A_1)$ into Some Element-Hydrogen Bonds

M. Koch, F. Temps, R. Wagener, and H. Gg. Wagner
Max-Planck-Institut für Strömungsforschung, Göttingen

Z. Naturforsch. **44a**, 195–204 (1989); received November 19, 1988

Absolute values for the removal rates of $CH_2(\tilde{a}\,^1A_1)$ by NH_3, CH_3NH_2, CH_3OH, HCl, and HF have been determined in the gas phase at low pressures and room temperature. $CH_2(\tilde{a}\,^1A_1)$ was generated by pulsed laser photolysis of CH_2CO. The measurements were carried out by observing the laser induced fluorescence of $^1CH_2$ after excitation by a pulsed laser as a function of the time delay between the photolysis and analysis pulses. The overall rate constants were found to be 2.4, 2.4, 2.3, 1.6 and $0.13 \cdot 10^{14}$ cm^3/mol s, respectively.

NH_2 was shown by LIF detection to be a primary product of the reaction of $^1CH_2$ with NH_3. The intersystem crossing channel of $^1CH_2$ was investigated by monitoring the formation of $CH_2(\tilde{X}\,^3B_1)$ with laser magnetic resonance. LMR absorption intensities of $^3CH_2$ resulting from quenching of $^1CH_2$ in the presence and absence of the reactant R were compared under otherwise identical conditions. The branching ratios of quenching versus total removal of $^1CH_2$ turned out to be 0.30, 0.13 and 0.98 for NH_3, CH_3OH, and HF, respectively.

1. Introduction

The insertion reactions of singlet methylene $CH_2(\tilde{a}\,^1A_1)$ (abbreviated as $^1CH_2$ throughout this paper) into C–H bonds have been investigated in some detail mainly by product analysis. Many measurements of collision stabilized insertion products have been carried out at different pressures to study unimolecular decomposition reactions of chemically activated aliphatic hydrocarbons [1]. In addition, the reactions of $^1CH_2$ with alkanes were studied in the high pressure regime with respect to unimolecular decomposition to determine relative insertion rate constants [2]. More recently, direct determination of rate constants of $^1CH_2$ reactions with several aliphatic hydrocarbons and H_2 [3, 4] have been performed using laser induced fluorescence (LIF) spectroscopy.

However, direct measurements of the reactivity of $^1CH_2$ towards element-hydrogen bonds other than C–H are comparatively rare. In a recent communication the results of measurements on the reaction system $^1CH_2 + H_2O$ were presented [5]. The scope of the work reported here is to extend direct kinetic investigation of $^1CH_2$ reactivity to the hydrogen bonds of the elements nitrogen, fluorine and chlorine. Furthermore, the reactions of $^1CH_2$ with methanol and methylamine were investigated.

Under low pressure conditions the reactions of $^1CH_2$ with H_2, CH_4 and H_2O lead to the formation of CH_3 [5, 6], probably by an insertion-decomposition mechanism. By analogy, the reaction of $^1CH_2$ with NH_3 should also form CH_3 and NH_2. Furthermore, a search for primary reaction products of the reaction $^1CH_2 + HF$ was carried out, because the high bond strength of HF leaves hardly any fragmentation channel accessible for the hypothetical insertion product CH_3F. These experiments were carried out in a quasi-static gas cell at low pressures using LIF detection of the radicals.

It is known that removal of $^1CH_2$ occurs partly by physical quenching leading to $^3CH_2$ [7]. In order to obtain information about the chemical reactivity of $^1CH_2$ towards a reactant R it is thus necessary to know the contribution of the physical deactivation channel

$$CH_2(\tilde{a}\,^1A_1) + R \rightarrow CH_2(\tilde{X}\,^3B_1) + R$$

to the total-removal rate of $^1CH_2$. Therefore, the formation of $^3CH_2$ in the reactions of $^1CH_2$ with the reactants NH_3, CH_3OH and HF was studied in a low-pressure flow-system. $^3CH_2$ was detected by laser magnetic resonance (LMR) absorption in the far infrared spectral region.

Reprint requests to Prof. Dr. H. Gg. Wagner, Max-Planck-Institut für Strömungsforschung, Bunsenstrasse 10, D-3400 Göttingen.

0932-0784 / 89 / 0300-0195 $ 01.30/0. – Please order a reprint rather than making your own copy.

2. Experimental

The experimental setup employed for the overall rate measurements has been described in detail earlier [8, 9, 10]. Briefly, a mixture of CH_2CO with He and the reactant R was photolyzed in a fluorescence cell, which was equipped with capacitance manometers (MKS Baratron, 0–10 Torr) and a gas supply system (Tylan, FC 280, RO 701 FC) providing a slow and constant gas flow. Thus the gas mixture was replaced between two laser shots so that reaction products did not accumulate.

The pulses of an XeCl excimer laser (Lambda Physik, EMG 101) at $\lambda_L = 308$ nm were employed for photolytic generation of methylene in its lowest singlet state with a quantum yield near unity [7, 11]. After a variable time delay, Δt, $^1CH_2$ was probed by detecting the LIF after excitation of the transition

$$CH_2(\tilde{b}\,^1B_1\ 0, 14, 0\ 4_{04} \leftarrow \tilde{a}\,^1A_1\ 0, 0, 0\ 4_{14})$$

at $\lambda = 590{,}71$ nm [12] with an excimer pumped dye laser (Lambda Physik, EMG 200, FL 3002). By means of a cut-off filter (Schott RG 630) the LIF signals were observed spectrally integrated by a photomultiplier (EMI 9816 QB) and stored by a transient digitizer (Tektronix 7912 AD). After averaging over 32–64 pulses the signals were integrated and processed further with a minicomputer (DEC, PDP 11/34).

The contributions of physical deactivation of $^1CH_2$ were investigated with an experimental setup similar to that described in [7, 13]. It consisted of a flow system with an intracavity LMR-Spectrometer. A Pyrex pipe of 4 cm diameter was used as flow tube in connection with a photolysis cell of 15 cm length and 4 cm diameter, equipped with a quartz window at one end and a dielectric mirror at the other end. For the LMR experiments with HF the complete Pyrex glass apparatus had to be replaced by a similar quartz flow-system to avoid blunting of the glass. The glass parts of both apparatus were rinsed with 5% HF solution prior to installation.

The photolysis cell was mounted parallel to the flow tube so that He, CH_2CO and the reactant, which were added through two inlets, passed into the LMR absorption cell simultaneously. Since the LMR cell was mounted a few cm below the photolysis cell and flow velocities were typically about 20 m/s, the residence time of the reactants usually was of the order of a few milliseconds.

In these experiments, UV-light pulses for photodissociating the CH_2CO were provided by an excimer laser (Lambda Physik, EMG 102) with pulse energy of 160 mJ at $\lambda_L = 308$ nm. The laser usually operated at a repetition frequency of 5 Hz so that no interference of concentration profiles of different laser pulses could occur. LMR-absorption of $^3CH_2$ was monitored with a CO_2-laser pumped $^{13}CH_3OH$ laser at $\lambda = 158$ μm and $B_0 = 0.323$ T in π-polarization [14]. The static magnetic field was modulated with 6 kHz. The absorption signals were detected with a Ge-Bolometer (Infrared Laboratories) and fed into a lock-in amplifier (EGG, time constant 3–10 ms) via a high pass filter (Geitmann, 4 kHz cut-off frequency). 50 to 500 signals were added using a transient recorder (Biomation) and a signal averager (Tracor Northern).

Chemicals with the highest commercial available purities were used without further purification. CH_2CO was prepared by pyrolysis of $(CH_3)_2CO$ and distilled from trap to trap ($T_1 = 77$ K, $T_2 = 195$ K) to purify it to >99%. It was stored at 77 K in the dark and dosed into the cells from a dry-ice cooled bulb during the experiments. Liquid reactants were evaporated in two stage thermostated saturators with He as carrier gas. HF was directly taken from its thermostated gas cylinder.

3. Results

3.1. $^1CH_2$ Removal Rates

$^1CH_2$ is produced by pulsed laser photolysis of CH_2CO:

$$CH_2CO + h\nu\,(\lambda = 308\text{ nm}) \rightarrow {}^1CH_2 + CO. \quad (1)$$

It is removed by reactions with the reactant R, He and CH_2CO:

$$^1CH_2 + R \xrightarrow{k_2(R)} \text{products}, \quad (2)$$

$$\xrightarrow{k_{2a}(R)} {}^3CH_2 + R, \quad (2a)$$

$$\xrightarrow{k_{2b}(R)} \text{chemical products}. \quad (2b)$$

$$^1CH_2 + He \xrightarrow{k_3} {}^3CH_2 + He, \quad (3)$$

$$k_3 = 2.0 \cdot 10^{12}\,\text{cm}^3/\text{mol s} \quad [3, 4]$$

$$^1CH_2 + CH_2CO \xrightarrow{k_{4a}} {}^3CH_2 + CH_2CO, \quad (4a)$$

$$\xrightarrow{k_{4b}} C_2H_4 + CO, \quad (4b)$$

$$k_4 = 1.5 \cdot 10^{14}\,\text{cm}^3/\text{mol s} \quad [4, 8].$$

Table 1. Total removal rates of $^1CH_2$ obtained in the pressure range given or taken from the references indicated.

R	$P_{min}(R)$ mbar	$P_{max}(R)$ mbar	$k_2(R)$ 10^{14} cm^3 mol^{-1} s^{-1}	
NH_3	0.004	0.058	2.4	this work
CH_3NH_2	0.006	0.056	2.4	this work
CH_3OH	0.009	0.072	2.3	this work
HCl	0.005	0.054	1.6	this work
HF	0.005	0.567	0.13	this work
H_2			0.78	[3]
CH_4			0.42	[4]
CH_4			0.44	[3]
H_2O			1.3	[5]

The experimental conditions were chosen such that the removal of $^1CH_2$ obeyed a first-order rate law. The pressure of He and CH_2CO were kept constant typically at $p(He)=1$ mbar and $p(CH_2CO)=3\cdot10^{-3}$ mbar during a series of measurements. Concentration-time profiles of $^1CH_2$ were recorded by means of LIF, varying the partial pressures of the reactants NH_3, CH_3NH_2, CH_3OH and HCl in the range $4\cdot10^{-3}$ mbar $\leqq p(R) \leqq 6\cdot10^{-2}$ mbar. The partial pressure of HF, which turned out to react about a factor of ten slower with $^1CH_2$ than the other reactants, was between 0.05 and 0.57 mbar. The excess of He, CH_2CO and R over $^1CH_2$ summed up to

$$([He]+[CH_2CO]+[R])/[^1CH_2]_{\Delta t=0} > 10^5,$$

because only several tenths of one per cent of CH_2CO were photolyzed by a single laser shot. Hence, consecutive reactions are negligible in the reaction scheme.

Semi-logarithmic plots of the LIF intensity of $^1CH_2$ versus time delay Δt yielded straight lines in the range $3\,\mu s \leqq \Delta t \leqq 8\,\mu s$. Signals were not analysed for $\Delta t < 3\,\mu s$, because the probed CH_2 level ($\tilde{a}\,^1A_1\,0,0,0\,4_{14}$) was populated by collisional relaxation during this period. Since $^1CH_2$ was removed very efficiently by most of the reactants, the signal/noise ratio for $\Delta t > 8\,\mu s$ became too low at the highest reactant pressures applied.

First order rate constant $k_{1.0.}$, when plotted versus reactant pressure $p(R)$, yielded straight lines with good linear correlation for all reactants. Plots of this kind are presented in Figure 1. The removal of $^1CH_2$ by He and CH_2CO leads to non-zero intercepts on the ordinate. Their values can be calculated from the known values for k_3 and k_4 [3, 4, 8], and the results agree well with the experimental data.

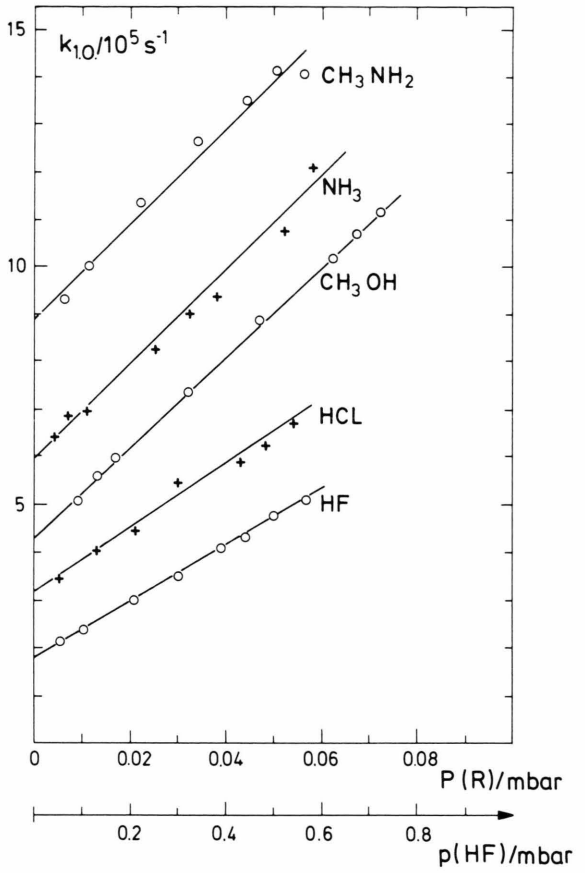

Fig. 1. Plots of the first order rate constants $k_{1.0.}$ versus reactant concentrations $p(R)$. Note that the abscissa has been compressed by a factor of ten for R = HF. The intercepts are about equal and around $1\cdot10^5\,s^{-1}$, but the lines have been displaced vertically for better comparison of the slopes.

The slopes of the graphs, which give the second order rate constants, were obtained from linear least squares fits. The second order rate constants are given in Table 1. The error limits quoted correspond to 2σ, twice the standard deviation of the linear least-squares slopes. For comparison, the rate constants for the reactions of $^1CH_2$ with H_2, CH_4 and H_2O taken from [3, 4, 5] are also shown in Table 1.

3.2. Physical Deactivation Rates

The contribution of physical quenching to the total removal of $^1CH_2$ was determined by comparison of the LMR absorption intensity of $^3CH_2$ in the presence and the absence of the reactant R under otherwise identical

Table 2. The contributions of physical deactivation to the removal of $^1CH_2$ by R determined under the experimental conditions indicated.

R	$\frac{p(R)_{min}}{mbar}$	$\frac{p(R)_{max}}{mbar}$	$\frac{p(He)}{mbar}$	m	$k_{2a}(R)/k_2(R)$
NH_3	0.025	0.680	2.00	35.56	0.30 ± 0.06
HF	0.116	0.572	2.00	5.89	0.98 ± 0.18
CH_3OH	0.137	0.292	1.15	14.26	0.13 ± 0.03

reaction conditions. In the absence of the reactant its flow was replaced by an equal flow of He in order to keep the flow-velocity and reaction time constant. However, the reactant was added between the photolysis cell and the LMR cell to keep the detection conditions constant. When no reactant R was present in the photolysis cell (indicated by $[^3CH_2]^-$ in the following), $^1CH_2$ was removed by reactions (3) and (4). When $^1CH_2$ was allowed to react with R (the notation $[^3CH_2]^+$ is used in this case) the reactions (2), (3) and (4) are competing.

In the data analysis it was assumed that the formation of $^3CH_2$ in channel (4a) can be neglected, because $[CH_2CO] \ll [He]$ (see below). Moreover, it was assumed that the photolysis of CH_2CO at $\lambda_L = 308$ nm leads exclusively [7, 11] to the formation of CH_2 in the singlet state. If these assumptions are not made, the data analysis becomes somewhat more involved, but does not cause substantial changes of the results, as is discussed in detail in [15]. Making allowance for $k_{4a}/k_4 = 0.25$, i.e. physical quenching of $^1CH_2$ by CH_2CO occurring with $k_{4a} = 4 \cdot 10^{13}$ cm^3/mol s [11, 15], causes a 10 percent relative increase of all ratios k_{2a}/k_2 determined and reported here as well as in [15]. Assuming quantum yields of $\Phi_1 = 0.9$ and $\Phi_3 = 0.1$ for the formation of $^1CH_2$ and $^3CH_2$, respectively, leads to a decrease of the ratios k_{2a}/k_2 of comparable magnitude. Hence, none of the assumptions can cause a systematic shift of the results which exceeds the experimental error quoted in Table 2.

The removal rates for $^3CH_2$ by most of the reactants used are much too slow to play a role within the time scale of the experiment. The recombination of two $^3CH_2$-radicals and consecutive reactions of $^3CH_2$ with fragmentation products of reaction channels (2b) are practically negligible due to the low concentrations. The reaction of $^3CH_2$ with CH_2CO has a rate constant of $k < 1 \cdot 10^9$ cm^3/mol s at room temperature [16] and also does not lead to a substantial removal of $^3CH_2$ in these experiments, since $[CH_2CO] \leqq 4 \cdot 10^{-10}$ mol/cm^3. Thus, the consumption of $^3CH_2$ is mainly due to wall reaction:

$$^3CH_2 + \text{wall} \xrightarrow{k_w} \text{products.} \qquad (5)$$

The wall removal rate constant is $k_w = (15 \pm 5)\ s^{-1}$, much slower than the rate of formation of $^3CH_2$. A continuous chemical source of $^3CH_2$ with variable position along the flow system was used to record concentration-time profiles of $^3CH_2$ in the presence of inert gases, and from these profiles the wall removal rate was calculated (more details are given in [13, 15]).

With these premises one obtains the following expression for $[^3CH_2]^+/[^3CH_2]^-$ at constant reaction time ($t \geqq 1$ ms) considering reactions (2) to (4) for $^3CH_2$-formation and neglecting removal reactions:

$$[^3CH_2]^+/[^3CH_2]^- = (k_D^+/k_T^+)/(k_D^-/k_T^-). \qquad (I)$$

The rates of total removal k_T and physical deactivation k_D of $^1CH_2$ in the presence "+" and the absence "−" of R are as follows:

$$k_D^+ = (k_{2a} - k_3)\,[R] + k_3\,[He]^-,$$

$$k_D^- = k_3\,[He]^-,$$

$$k_T^+ = (k_2 - k_3)\,[R] + k_3\,[He]^- + k_4\,[CH_2CO],$$

$$k_T^- = k_3\,[He]^- + k_4\,[CH_2CO].$$

Here, $[He]^-$ is the concentration of He in the absence of R and $[He]^+$ that with R present. In the experiments $[He]^- = [He]^+ + [R]$. k_{2a} is the rate constant for physical quenching of $^1CH_2$ by R to be determined. The physical quenching of $^1CH_2$ by CH_2CO has been neglected for the reasons given above.

Equation (I) can be rearranged and analysed in terms of the linear equation

$$\gamma = \left(\frac{[^3CH_2]^+}{[^3CH_2]^-}\,\frac{k_T^+}{k_T^-}\right) = \frac{k_D^+}{k_D^-} = 1 + \frac{k_{2a} - k_3}{k_3}\,\frac{[R]}{[He]^-}$$

$$= 1 + m\,\frac{[R]}{[He]^-}. \qquad (II)$$

γ can be determined from known quantities. Plots of γ versus $[R]/[He]^-$ yield straight lines with an intercept $\gamma(0) = 1$ according to (II). This is shown in Figure 2. From the slopes m of the lines the rate of physical deactivation is obtained as $k_{2a} = (m+1)\,k_3$. The ratios of physical deactivation to the total removal rates of $^1CH_2$ determined in this manner are presented in Table 2.

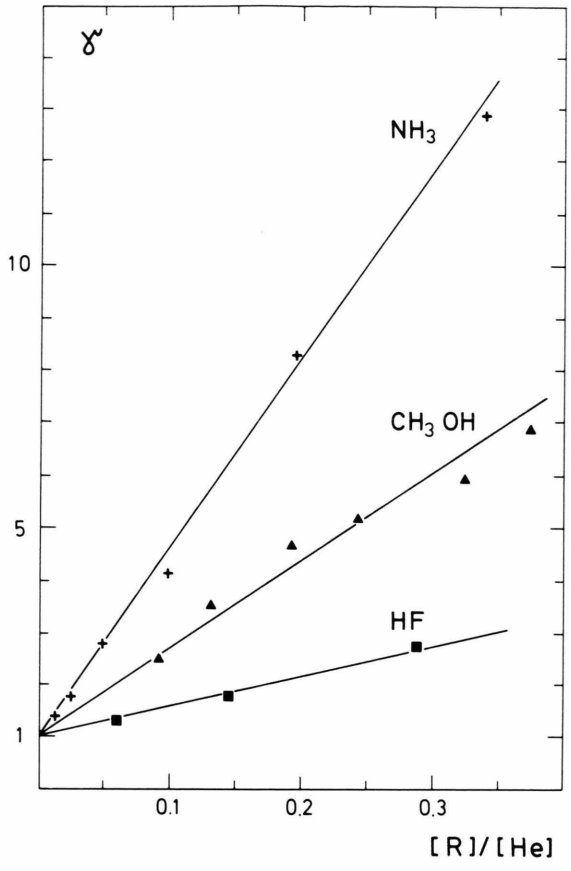

3.3. *Product Analysis of the Reaction* $^1CH_2 + NH_3$

In the reaction of $^1CH_2$ with NH_3, NH_2-radicals were identified by LIF. No fluorescence signals of NH_2 were observed in the absence of either CH_2CO or NH_3 in the gas cell, nor did NH_2 result from a dark reaction of these components because it was observed only after a photolysis laser pulse. The reaction of $^3CH_2$ with NH_3 is too slow to play a role.

Concentration profiles of $^1CH_2$ and NH_2 were recorded in two consecutive experimental runs at $p(NH_3) = 0.016$ mbar, $p(He) = 1$ mbar and $p(CH_2CO) = 4 \cdot 10^{-3}$ mbar to ensure that the reaction conditions in the gas cell were identical for both profiles. It was confirmed that the excitation line $^RQ_{O,N}$ (4) of the transition NH_2 ($\tilde{A}\ ^2A_1$ 0, 10, 0 – $\tilde{X}\ ^2B_1$ 0, 0, 0) near 570.7 nm [17] did not interfere with anyone of the numerous lines of $^1CH_2$ in this spectral region.

The profiles of $^1CH_2$ and NH_2 shown in Fig. 3 are normalized with respect to the observed maximum fluorescence intensity I_{max} but not with respect to each

Fig. 2. Plots of γ versus [R]/[He]$^-$. From the slope $m = (k_{2a} - k_3)/k_3$ the rates of physical quenching of $^1CH_2$ by R, k_{2a}, were obtained. The intercepts are $\gamma(0) = 1$ according to (II).

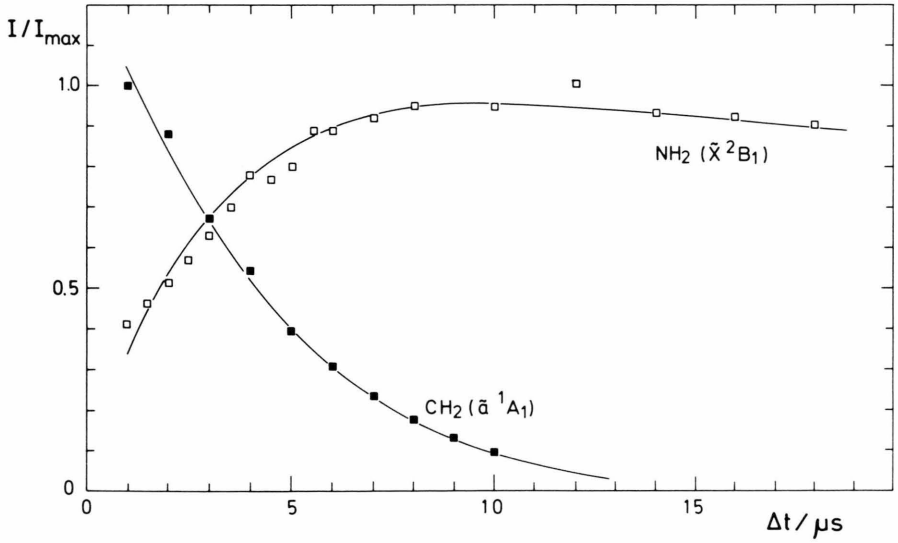

Fig. 3. Profiles of the reduced fluorescence intensities of $^1CH_2$ and NH_2 as a function of reaction time. The profiles were analyzed in terms of a first order rate law as described in the text.

other. They were analyzed in terms of a first order rate law. The first order rate constant for the removal of $^1CH_2$ was determined from a semi-logarithmic plot of the $^1CH_2$ fluorescence intensity versus Δt to be

$$k_{1.0.}(^1CH_2) = (2.7 \pm 0.1) \cdot 10^5\ s^{-1}.$$

After taking into account the slow disappearance of NH_2 due to diffusion and reaction with CH_2CO, the NH_2 profile could also be evaluated by plotting $\ln(1 - I/I_{max})$ versus Δt. Here I represents the fluorescence intensity of the NH_2 present at time t. A straight line was obtained from this plot, leading to a rate constant

$$k_{1.0.}(NH_2) = (3.0 \pm 0.4) \cdot 10^5\ s^{-1}$$

in the time range of 2–5 μs. Within experimental error the intercept of the line is zero. These rate constants are in good agreement with the data obtained in the measurements reported in Table 1. It is concluded that NH_2 is a primary product of the reaction $^1CH_2 + NH_3$.

4. Discussion

4.1. Discussion of the Reactions Investigated in this Work

4.1.1. $^1CH_2 + NH_3$

The reaction

$$^1CH_2 + NH_3 \rightarrow \text{prod.} \qquad (6)$$

has been found to be one of the fastest reactions of $^1CH_2$ with k_6 very close to the rate constants for the removal of $^1CH_2$ by unsaturated hydrocarbons [18, 19]. The removal of $^1CH_2$ by NH_3 is mainly due to chemical reaction, whereas the contribution of physical quenching is $k_{6a}/k_6 = 0.30$.

The NH_2-radical was detected as one of the primary chemical reaction products. In principle it could arise by direct abstraction or by an insertion-decomposition mechanism. There is some reason to prefer the reaction pathway of N–H insertion and subsequent decomposition of chemically activated methylamine: Chao et al. [20] and Ho et al. [21] have shown by analysis of the collision stabilized product of (6) that in the high pressure regime formation of the insertion product methylamine CH_3NH_2 is the main pathway of (6). Other products, which could be interpreted as consecutive products from competing reaction steps given below, have been detected only in trace amounts, as reported in [21]. The measured pressure dependence of the yield of CH_3NH_2 was reproduced by Chao et al. [20] with RRKM-calculations of the unimolecular decay of chemically activated methylamine. Moreover, NH_2 is known to be a major product of the thermal unimolecular decomposition of CH_3NH_2 [22]. This follows also from IR-multiphoton excitation under collision-free conditions [23]. Thus, decomposition of chemically activated methylamine is the most probable reaction path to form NH_2 in (6).

The following scheme shows that there are further exothermic reaction pathways besides physical quenching and formation of NH_2 (thermodynamic data taken from [5, 24, 25]):

$$^1CH_2 + NH_3 \rightarrow$$

$$\rightarrow {}^3CH_2 + NH_3, \qquad \Delta H_r = -\ 38\ \text{kJ/mol}, \qquad (6a)$$

$$\rightarrow [CH_3NH_2]^*, \qquad \Delta H_r = -406\ \text{kJ/mol}, \qquad (6b)$$

$$\rightarrow CH_2NH_2 + H, \qquad \Delta H_r = -\ 15\ \text{kJ/mol}, \qquad (6c)$$

$$\rightarrow CH_3NH + H, \qquad \Delta H_r = -\ 25\ \text{kJ/mol}, \qquad (6d)$$

$$\rightarrow CH_3 + NH_2, \qquad \Delta H_r = -\ 70\ \text{kJ/mol}, \qquad (6e)$$

$$\rightarrow CH_2NH + H_2, \qquad \Delta H_r = -273\ \text{kJ/mol}, \qquad (6f)$$

$$\rightarrow CH_4 + NH(X^3\Sigma), \qquad \Delta H_r = -118\ \text{kJ/mol}, \qquad (6g)$$

$$\rightarrow CH_4 + NH(a^1\Delta), \qquad \Delta H_r = +\ 32\ \text{kJ/mol}. \qquad (6h)$$

Reaction (6e), however, remains the most exothermic channel resulting from simple bond breaking of $[CH_3NH_2]^*$, whereas reaction channels (6f) and (6g) require a more complicated rearrangement of the molecular frame and thus probably an additional activation energy.

4.1.2. $^1CH_2 + CH_3NH_2$

The reaction

$$^1CH_2 + CH_3NH_2 \rightarrow \text{prod.} \qquad (7)$$

allows a comparison of the insertion rates into C–H and N–H bonds. Its rate k_7 is identical with k_6. No exact determination of the physical quenching rate is available for CH_3NH_2. It can be estimated in analogy with the quenching rates of NH_3, H_2O, CH_3OH and several hydrocarbons [5, 13, 18, 19] that chemical reaction pathways are the major ones in (7). A gas chromatographic investigation of collision stabilized products of (7) yielded $(CH_3)_2NH$ and $C_2H_5NH_2$ as major compounds [21]. The results of this product

analysis were interpreted in terms of competitive insertion of $^1CH_2$ into C–H and N–H bonds followed by unimolecular decay of the resulting chemically activated $[C_2H_7N]^*$ molecule. The ratio of the products $[(CH_3)_2NH]/[C_2H_5NH_2]$ was found to be nearly independent of pressure ($30 \leqq p/\text{mbar} \leqq 670$) [21]. It corresponds to the statistical ratio 3:2 of the numbers of C–H bonds and N–H bonds in CH_3NH_2. Thus, the rate constants for $^1CH_2$ insertion into a methyl H–C and an H–N bond should be nearly equal.

4.1.3. $^1CH_2 + CH_3OH$

The rate constant k_8 of the reaction

$$^1CH_2 + CH_3OH \rightarrow \text{prod.} \qquad (8)$$

is found to be nearly identical with that of the reactions of $^1CH_2$ with NH_3 and CH_3NH_2, but slightly faster than that with H_2O [5] (see Table 1). Physical quenching is found to be less effective in the case of methanol, $k_{8a}/k_8 = 0.13$, than in the case of NH_3 and H_2O [5].

The products of (8) are known to be CH_3OCH_3 and C_2H_5OH [26–28]. They should result from competing $^1CH_2$ insertion into C–H and O–H bonds as in the analogous case of CH_3NH_2. Ogoshi and Takezaki [28] determined C–H insertion to be about 2.5 times faster than O–H insertion. However, their experiments suffered from a dark reaction of the methylene precursor ketene with methanol. Kerr et al. [26] found by gas chromatographic analysis that the O–H bond of CH_3OH was about 22 times more reactive towards insertion of $^1CH_2$ than a single C–H bond of the CH_3 group. This agrees reasonably well with the result of Ho and Lin [27], who stated the O–H bond to be about 33 times more reactive. In addition they found that $^1CH_2$ inserts into the O–H bond of C_2H_5OH 21 times faster than into the primary and 28 times faster than into the secondary C–H bond. It is assumed here that the results of [27, 26] are correct and that the rate of O–H insertion is about a factor of 25 higher than the rate of C–H insertion for (8).

4.1.4. $^1CH_2 + HF$

The reaction

$$^1CH_2 + HF \rightarrow \text{prod.} \qquad (9)$$

is found to be slower by a factor of about ten than the reactions of $^1CH_2$ with NH_3, H_2O and HCl. The investigation of the physical deactivation channel shows that the physical quenching rate is practically identical with the total removal rate, so that the removal of $^1CH_2$ in (9) seems to proceed exclusively via formation of $^3CH_2$. The following scheme illustrates that there are possibly two thermodynamically allowed product channels, accessible either directly or via fragmentation of an activated CH_3F-molecule, formed by insertion of $^1CH_2$ into the H–F bond:

$$CH_2(\tilde{a}\,^1A_1) + HF \rightarrow$$

$$\rightarrow CH_2(\tilde{X}\,^3B_1) + HF, \quad \Delta H_r = -38\ \text{kJ/mol}, \qquad (9a)$$

$$\rightarrow [CH_3F]^*, \quad \Delta H_r = -389\ \text{kJ/mol}, \qquad (9b)$$

$$\rightarrow CH_3 + F, \quad \Delta H_r = +69\ \text{kJ/mol}, \qquad (9c)$$

$$\rightarrow CH_2F + H, \quad \Delta H_r = +30\ \text{kJ/mol}, \qquad (9d)$$

$$\rightarrow CHF(\tilde{X}\,^1A') + H_2, \qquad (9e)$$

$$-50 \leqq \Delta H_r/\text{kJ mol}^{-1} \leqq +10.$$

The thermodynamic data have been taken from [5, 24, 29]. As a consequence of the extraordinary high bond strength of HF, reaction channel (9c) is clearly endothermic, whereas the analogous reaction channels are exothermic for the reactions of $^1CH_2$ with CH_4, NH_3 and HCl and nearly thermoneutral for H_2O [5]. A similar situation is encountered for the reaction channel (9d).

There is some uncertainty about the heat of formation of monofluorocarbene CHF formed in (9e) [29]. Reaction (9e) may be exothermic, or it may be slightly endothermic. With the value $\Delta H_f(CHF) = (109 \pm 12)$ kJ/mol, recommended by Lias et al. [29] based on a detailed discussion of recent theoretical and experimental results, the reaction should be exothermic. Therefore it was checked if CHF could be detected in the reaction mixture by LIF in the spectral region given in [8, 30]. In agreement with the finding that $k_{9a}/k_9 = 0.98$, no LIF signals of CHF could be recorded, even if a pure mixture of CH_2CO ($p = 0.038$ mbar) and HF ($p = 0.43$ mbar) was used. With the assumptions that the detection limit of CHF given in [8] for the experimental set up used here, and the photodissociation yield for CH_2CO, determined in this laboratory under practically identical experimental conditions in [9], are applicable also in the present experiments, one can estimate an upper limit for k_{9e}, the α–α elimination of H_2. Assuming further that the reaction

$$CHF(\tilde{X}) + CH_2CO \rightarrow \text{prod.} \qquad (10)$$

is the most important reaction for the removal of CHF under the conditions applied one obtains the relation:

$k_{9e} \leqq 0.013\, k_{10}$. With $k_{10} = 1.0 \cdot 10^{14}$ cm^3/mol s as an upper limit, this means that $k_{9e}/k_9 < 0.1$.

Thus channel (9a) is the only important exothermic pathway, occurring either directly by collision-induced intersystem crossing or by non-adiabatic decomposition of $[CH_3F]^*$. Reaction (9b) should, according to ab initio calculations [31, 32], occur without any barrier in the reaction coordinate. However, hardly any $[CH_3F]^*$ can be stabilized under the conditions applied here. The reverse reaction $CH_3F \rightarrow {}^1CH_2 + HF$ may compete with the non-adiabatic decomposition $CH_3F \rightarrow {}^3CH_2 + HF$. This would require $k_{9a} \ll k_{-9b}$. Another possibility for the low k_9 would be that the high H–F bond energy reduces the rate of the insertion step, as indicated by the results available with other reactants, so that it drops to or below a rate constant for a process which does not proceed via a $[CH_3F]^*$ complex. In the latter case one may ask why its rate constant is relatively low compared to physical deactivation of $^1CH_2$ by other reactants. A decision should be possible as in other cases [15] by experiments with isotopically substituted reactants.

4.1.5. $^1CH_2 + HCl$

The rate of the reaction

$$^1CH_2 + HCl \rightarrow \text{prod.} \qquad (11)$$

is found to be about as fast as the reactions of $^1CH_2$ with H_2O and NH_3 (see Table 1). The experiments indicated that the reaction

$$^3CH_2 + HCl \rightarrow \text{prod.} \qquad (12)$$

is also relatively fast, so that the physical quenching rate could not be determined with the technique used here.

The major chemical reaction channel of (11) is assumed to be insertion of $^1CH_2$ and subsequent decomposition of $[CH_3Cl]^*$. The possible reaction channels are given below (with thermochemical data taken from [5, 24, 29]):

$$^1CH_2 + HCl \rightarrow$$

$$\rightarrow {}^3CH_2 + HCl, \quad \Delta H_r = -\ 38 \text{ kJ/mol}, \qquad (11a)$$

$$\rightarrow [CH_3Cl]^*, \quad \Delta H_r = -419 \text{ kJ/mol}, \qquad (11b)$$

$$\rightarrow CH_3 + Cl, \quad \Delta H_r = -\ 70 \text{ kJ/mol}, \qquad (11c)$$

$$\rightarrow CH_2Cl + H, \quad \Delta H_r = +\ 7 \text{ kJ/mol}, \qquad (11d)$$

$$\rightarrow HCCl + H_2, \quad \Delta H_r = -\ 37 \text{ kJ/mol}. \qquad (11e)$$

All decomposition channels of $[CH_3Cl]^*$ are thermochemically allowed. Reaction (11c) seems to be a logical pathway in the low pressure region, in analogy with the reactions of $^1CH_2$ with H_2, CH_4, NH_3 and H_2O. Experiments about the thermal dissociation of CH_3Cl behind shock waves indicate that C–Cl bond fission (11c) is the dominating initiation reaction, whereas the elimination of HCl (11a) or H_2 (11e) probably do not play a role [33].

4.2. Comparative Discussion of $^1CH_2$ Insertion Reactions

The results shown in Table 1 on reactions of $^1CH_2$ with hydrogen bearing compounds exhibit some interesting details. Clearly, the reactions of $^1CH_2$ with NH_3, CH_3NH_2, CH_3OH, HCl and H_2O cannot require activation energies because the reaction rates are very close to that for the gas kinetic collision frequency. An exception is the reaction of $^1CH_2$ with HF, as discussed in Section 4.1.4. The comparatively slow removal rate of $^1CH_2$ by CH_4 is puzzling. Exothermic reaction channels are well known, and among the simple hydrids considered here, methane provides the maximum number of insertion reaction sites, i.e. number of hydrogen atoms. Nevertheless, its cross section for removal of $^1CH_2$ is the second smallest among the molecules CH_4, NH_3, H_2O, HCl and HF.

Secondly, there is the finding that insertion of $^1CH_2$ into the O–H bonds of CH_3OH and C_2H_5OH is about 25 times faster than the insertion into the C–H bonds, whereas in the case of CH_3NH_2 the corresponding insertion reactions per bond have comparable rates. This is rather surprising if one remembers that insertion into O–H and N–H bonds of the parent compounds H_2O and NH_3 occurs at about the same rate.

A qualitative explanation of these findings may be derived considering recent experimental [34] and theoretical [31, 32, 35–37] studies on simple ylides. There is agreement between the theoretical and experimental investigations [32, 34] that the methyleneammonium ylide $H_2C{-}NH_3$ is located in a minimum of the CH_3NH_2 potential energy surface. The activation energy of the ylide-isomerization leading to CH_3NH_2 is smaller than the dissociation energy necessary to form $^1CH_2$ and NH_3, as reported in [32]. The conclusion drawn by Pople et al. [32] is, that insertion of $^1CH_2$ into N–H bonds of NH_3 should occur without activation energy. Thus one may interpret the primary

reaction step as "electrophilic attack" of $^1CH_2$ on the non-bonded electron pair of NH_3, yielding the methyleneammonium ylide, followed by rearrangement to CH_3NH_2. From this point of view the similarity of the cross sections (about 40 Å^2) for reactions of NH_3 and non-saturated hydrocarbons [18, 19] in the removal of $^1CH_2$ is explained by analogous interaction forces.

However, theory and experiment do not agree so well about the stability of the methyleneoxonium- and the methylenechloronium-ylide. Ab initio calculations predict no stabilization of $^1CH_2$ by ylide formation with HCl [37]. A very small stabilization energy of about 0–20 kJ/mol [32, 35] was calculated for the ylide-formation by $^1CH_2$ and H_2O. No barriers were found for the isomerization of the corresponding ylides to CH_3Cl [37] and CH_3OH [32], respectively.

In contrast, the ylide-forms of CH_3Cl and CH_3OH were shown experimentally to be in a local potential surface minimum. This result was derived by means of neutralization-reionization mass spectrometry [34]. Thus the interaction of $^1CH_2$ with H_2O and HCl may parallel that with NH_3, and an "electrophilic attack" on the lone electron pairs of Cl and O by $^1CH_2$ may occur. A mechanism of this type has been employed by several authors to explain the results of gas-chromatographic product analyses of the reaction of $^1CH_2$ with alkylchlorides [38] and ethers [39], and it has also been demonstrated to be plausible in a quantum mechanical study for the reaction with CH_3Cl [40]. Obviously this type of primary reaction step cannot occur for the reaction of $^1CH_2$ with CH_4, since no lone electron pair is available in methane. This may be the reason why the reaction of $^1CH_2$ with CH_4 is distinctly slower than that with NH_3, H_2O and HCl.

The case of HF is, here again, somewhat different. Experimental [34] and theoretical [31] studies do agree that an adduct of $^1CH_2$ and HF is thermodynamically stable against decomposition and that a certain barrier, albeit very low, exists for the isomerization reaction leading to CH_3F. However, the results of the ab initio calculations [31] show that this adduct is not a methylenefluoronium-ylide H_2C-FH but a hydrogen-bonded H_2C-HF. Consequently this species would result from a nucleophilic attack of $^1CH_2$ on HF. This qualitative difference in the interactions of $^1CH_2$ with HF in contrast to NH_3, H_2O and HCl may cause substantial differences in the cross sections and provide a quite natural mechanistic explanation for the rate constants determined in this work.

On the basis of the model of ylide formation by electrophilic attack of $^1CH_2$ on lone electron pairs one can understand why insertion into the O–H bond of CH_3OH is fast compared to C–H insertion, whereas N–H and C–H insertions are nearly equally fast for CH_3NH_2. As a result of the electrophilic attack on the oxygen atom by $^1CH_2$, leading to oxygen lone pair donation into a vacant orbital on the carbon [35], the polarity of the O–H bond may be enhanced. This may cause Coulombic attraction forces between the oxygen bonded hydrogen, bearing a partial positive net charge, and the methylene carbon, which acts as electron acceptor. Hence O–H insertion is preferred to C–H insertion in this simple qualitative interpretation of the ab initio calculations. Since CH_3NH_2 is a much weaker protic acid than CH_3OH, due to the greater electronegativity of oxygen compared to nitrogen, this argument perhaps fails in the case of the ylide formed by $^1CH_2$ and CH_3NH_2. Instead, random attack of the methylene group may lead to C–H and N–H insertion products in the statistical ratio as observed experimentally.

Acknowledgement

We wish to thank Dr. W. Hack for helpful discussions during the course of this work.

[1] W. L. Hase and J. W. Simons, J. Chem. Phys. **54,** 1277 (1971). – R. L. Johnson, W. L. Hase, and J. W. Simons, J. Chem. Phys. **52,** 3911 (1970). – G. Z. Whitten and B. S. Rabinovitch, J. Phys. Chem. **69,** 4348 (1965). – J. N. Butler and G. B. Kistiakowsky, J. Amer. Chem. Soc. **82,** 759 (1970); **83,** 1324 (1961). – H. M. Frey, Proc. Chem. Soc. London **1959,** 318. – H. M. Frey and G. B. Kistiakowsky, J. Amer. Chem. Soc. **79,** 6373 (1957). – D. F. Ring and B. S. Rabinovitch, Can. J. Chem. **46,** 2435 (1968).

[2] M. L. Halberstadt and J. Crump, J. Photochem. **1,** 295 (1972) and references therein. – W. Kirmse, Carbene Chemistry, 2nd ed., New York 1971 and references therein.

[3] M. N. R. Ashfold, M. A. Fullstone, G. Hancock, and G. W. Ketley, Chem Phys. **55,** 245 (1981).

[4] A. O. Langford, H. Petek, and C. B. Moore, J. Chem. Phys. **78,** 6650 (1983).

[5] W. Hack, H. Gg. Wagner, and A. Wilms, Ber. Bunsenges. Phys. Chem. **92,** 620 (1988).

[6] G. Herzberg, Proc. Roy. Soc London A **262,** 291 (1961). – J. A. Bell and G. B. Kistiakowsky, J. Amer. Chem. Soc. **84,** 3417 (1962). – P. Ausloos, R. Gorden Jr., and S. G. Lias, J. Chem. Phys. **40,** 1854 (1964). – W. Brown, A. M. Bass, and M. Pilling, J. Chem. Phys. **52,** 5131 (1970).

[7] T. Böhland, F. Temps, and H. Gg. Wagner, Ber. Bunsenges. Phys. Chem. **89,** 1013 (1985).

[8] G. Dornhöfer, Dissertation, MPI f. Strömungsforschung, report 3/85, Göttingen 1985.
[9] A. Wilms, Dissertation, MPI f. Strömungsforschung, report 3/87, Göttingen 1987.
[10] W. Hack and A. Wilms, J. Phys. Chem. **93,** 1923 (1989).
[11] R. Becerra, L. E. Canosa-Mas, H. M. Frey, and R. Walsh, J. Chem. Soc. Faraday Trans. 2, **83,** 435 (1987). – C. C. Hayden, D. M. Neumark, K. Shobatake, R. K. Sparks, and Y. T. Lee, J. Chem. Phys. **76,** 3607 (1982). – I. C. Chen, W. H. Green, and C. B. Moore, J. Chem. Phys. **89,** 314 (1988).
[12] G. Herzberg and J. W. C. Johns, Proc. Roy. Soc. London A **295,** 107 (1966). – H. Petek, D. J. Nesbitt, D. C. Darwin, and C. B. Moore, J. Chem. Phys. **86,** 1172 (1987).
[13] T. Böhland, Dissertation, MPI f. Strömungsforschung, report 18/86, Göttingen 1986.
[14] T. J. Sears, P. R. Bunker, A. R. W. McKellar, K. M. Evenson, D. A. Jennings, and J. M. Brown, J. Chem. Phys. **77,** 5348 (1982).
[15] M. Koch, Dissertation, Göttingen 1988.
[16] P. S. T. Lee, R. L. Russell, and F. S. Rowland, Chem. Commun. **1970,** 18.
[17] K. Dressler and D. A. Ramsay, Philos. Trans. Roy. Soc. London **A 251,** 553 (1959).
[18] W. Hack, M. Koch, H. Gg. Wagner, and A. Wilms, Ber. Bunsenges. Phys. Chem. **92,** 674 (1988).
[19] M. Koch and R. Wagener, MPI f. Strömungsforschung, report 12/88. – W. Hack, M. Koch, R. Wagener, and H. Gg. Wagner, Ber. d. Bunsenges. Phys. Chem. **93,** 261 (1989).
[20] K. J. Chao, C. L. Lin, M. Hsu, and S. Y. Ho, J. Phys. Chem. **83,** 1241 (1979).
[21] S. Y. Ho and S. N. Tong, J. Chin. Chem. Soc. (Taipeh) **19,** 189 (1972).
[22] E. Maier, Dissertation, Göttingen 1972. – T. Higashihara., W. C. Gardiner Jr., and S. M. Hwang, J. Phys. Chem. **91,** 1900 (1987).
[23] S. V. Filseth, J. Danon, D. Feldmann, J. D. Campbell, and K. H. Welge, Chem. Phys. Lett. **63,** 615 (1979). – R. Schmiedl, R. Böttner, H. Zacharias, U. Meier, and K. H. Welge, Opt. Comm. **31,** 329 (1979). – G. Hancock, R. J. Hennessey, and T. Villis, J., Photochem. **10,** 305 (1979). – D. K. Evans, R. D. McAlpine, H. M. Adams, and A. L. Creagh, Chem. Phys. **80,** 379 (1983).
[24] JANAF Thermochemical Tables (R. Stuhl and H. Prophet, eds.), 2nd ed., N.B.S. Washington 1971. – S. W. Benson, Thermochemical Kinetics, 2nd ed., John Wiley & Sons, New York 1976. – CRC Handbook of Chemistry and Physics, 65th ed., R.C. Weast Ed., Boca Raton 1985.
[25] M. A. Grela and A. J. Colussi, Int. J. Chem. Kin. **20,** 713 (1988). – P. Rouveirolles, These de Doctorat de 3eme Cycle, Göttingen 1985. – D. J. De Frees and W. J. Hehre, J. Phys. Chem. **82,** 391 (1978).
[26] J. A. Kerr, B. V. O'Grady, and A. F. Trotman-Dickson, J. Chem. Soc. (A) **1967,** 857.
[27] S. Y. Ho and H. B. Lin, J. Chin. Chem. Soc. (Taipeh) **20,** 27 (1973).
[28] H. Ogoshi and Y. Takezaki, Bull. Inst. Chem. Res., Kyoto Univ. **38,** 299 (1960).
[29] S. G. Lias, Z. Karpas, and J. F. Liebmann, J. Amer. Chem. Soc. **107,** 6089 (1985).
[30] M. N. R. Ashfold, F. Castano, G. Hancock, and G. W. Ketley, Chem. Phys. Lett. **73,** 421 (1980).
[31] J. A. Pople, Chem. Phys. Lett. **132,** 144 (1986).
[32] J. A. Pople, K. Raghavachari, M. J. Frisch, J. S. Binkley, and P. v. R. Schleyer, J. Amer. Chem. Soc. **105,** 6389 (1983).
[33] O. Kondo, K. Saito, and I. Murakami, Bull. Chem. Soc. Japan **53,** 2133 (1980). – A. E. Shilov and R. D. Sabirova, Z. Fiz. Khim. **33,** 1365 (1959).
[34] C. Wesdemiotis, R. Feng, P. O. Davis, E. R. Williams, and F. W. McLafferty, J. Amer. Chem. Soc. **108,** 5847 (1986).
[35] D. A. Dixon, T. H. Dunning, R. A. Eades, and P. G. Gassmann, J. Amer. Chem. Soc. **105,** 7011 (1983).
[36] R. A. Eades, P. G. Gassmann, and D. A. Dixon, J. Amer. Chem. Soc. **103,** 1066 (1981).
[37] B. F. Yates, W. J. Bouma, and L. Radom, J. Amer. Chem. Soc. **106,** 5805 (1984).
[38] C. H. Bamford and J. E. Casson, Proc. Roy. Soc. London A **289,** 287 (1966); **306,** 135 (1968); **312,** 141 (1969). – R. L. Johnson and D. W. Setser, J. Phys. Chem. **71,** 4366 (1967). – J. C. Hassler and D. W. Setser, J. Chem. Phys. **45,** 3237 (1966). – W. G. Clark, D. W. Setser, and E. E. Siefert, J. Phys. Chem. **74,** 1670 (1970).
[39] H. M. Frey and M. A. Voisey, Trans. Faraday Soc. **64,** 954 (1968). – W. Kirmse and M. Buschhoff, Chem. Ber. **102,** 1087, 1098 (1969).
[40] S. P. Kolesnikov, A. I. Ioffe, and O. M. Nefedov, Izv. Akad. Nauk, SSSR, Ser. Khim. **1973,** 2622.